Technical University of Denmark

Raman Spectroscopic Study of the Vapour Phase of 1-Methylimidazolium Ethanoate, a Protic Ionic Liquid

Berg, Rolf W.; Canongia Lopes, Jose N.; Ferreira, Rui; Rebelo, Luis P. N.; Seddon, Kenneth R.; Tomaszowska, Alina A.

Link back to DTU Orbit

DTU Library
Technical Information Center of Denmark

Raman Spectroscopic Study of the Vapor Phase of 1-Methylimidazolium Ethanoate, a Protic Ionic Liquid

Rolf W. Berg,*,† José N. Canongia Lopes,‡ Rui Ferreira,‡ Luís Paulo N. Rebelo,‡ Kenneth R. Seddon,‡,§ and Alina A. Tomaszowska§,⊥

Department of Chemistry, Technical University of Denmark, Building 207, Kemitorvet, DK-2800 Kgs. Lyngby, Denmark, Instituto de Tecnologia Química e Biológica, Universidade Nova de Lisboa, Av. República, Apartado 127, 2780-901 Oeiras, Portugal, The QUILL Centre, The Queen's University of Belfast, Stranmillis Road, Belfast BT9 5AG, U.K., and Department of Materials Science & Engineering, Massachusetts Institute of Technology, 77 Massachusetts Avenue, 4-217, Cambridge, Massachusetts 02139

The gas phase over the ionic liquid 1-methylimidazolium ethanoate, [Hmim][O$_2$CCH$_3$], was studied by means of Raman spectroscopy. Raman spectra are presented, the species in the gas phase are identified, and their bands are assigned. The results are interpreted using ab initio quantum mechanical calculations that also predict vibrational spectra. The obtained data reinforce a previous interpretation, based on FT-ICR mass spectrometric data, that the vapor phase over [Hmim][O$_2$CCH$_3$] consists predominantly of two neutral molecules, monomeric ethanoic acid and 1-methylimidazole.

Introduction

Salts which are liquid at about room-temperature, namely, ionic liquids, can be grouped into two classes, (i) aprotic ionic liquids, which are solely composed of ions, and (ii) protic ionic liquids, where the cations ([BH]$^+$) and anions (A$^-$) are able to exchange a proton with each other. In the latter case, a dynamic equilibrium with the formation of two neutral species (the conjugate base, B, and acid, AH), which are derived solely from the salt, is established (eq 1).[1−3]

$$[BH]^+ + A^- \rightleftharpoons B + AH \qquad (1)$$
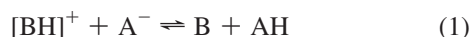
Both classes represent situations which are totally distinct from ionic solutions (even the latter one) as in ionic solutions, there exists a molecular solvent which is chemically dissimilar from the solute ions, and this solvent can, for instance, evaporate "independently" of the ions. The distinction between aprotic and protic ionic liquids is not clear-cut. Some protic ionic liquids present such a low equilibrium constant for eq 1 that, in practice, they are effectively fully ionized; others have such a high equilibrium constant that they are effectively a mixture of two molecular species.[1] Many authors (e.g., refs 2, 3, 6, and 7) even coined the terms "strong" and "poor" ionic liquids to describe the extremes of these two situations.

While most ionic liquids have extremely low vapor pressures, even at moderately high temperatures,[4,5] some ionic liquids, specifically the protic ones, present measurable vapor pressures, some even at room temperature or lower.[3,6] Moreover, their vapor pressures, and consequently their boiling points, strongly depend on the overall composition of the liquid, as determined by the equilibrium constant of eq 1.[6]

Due to their general stability, nonflammability, amphiphilic nature, low volatility (in the case of aprotic ionic liquids), and the possibility to tune their physical properties simply by changing the anion and/or cation, ionic liquids have found a broad range of applications in many disparate fields of research, as well as in industry.[1,8] On the fundamental side, since the recent surprising demonstration[4] that even aprotic ionic liquids, which present no measurable vapor pressure under ambient conditions, could be distilled, many studies have been dedicated to determine the constitution of their vapor phases, being based on a wide range of mass spectrometric (MS) techniques. For instance, on the basis of Fourier transform ion cyclotron resonance (FT-ICR) MS measurements, Leal et al.[9] concluded that an ionic liquid such as 1-methylimidazolium ethanoate, [Hmim][O$_2$CCH$_3$], distills under reduced pressure as two volatile neutral molecules (the acid and the base). On the other hand, Berg et al.[10] in a recent Raman study of the protic salt 1,1,3,3-tetramethylguanidinium chloride, [{(CH$_3$)$_2$N}$_2$CNH$_2$]Cl or [tmgH]Cl, obtained results which might indicate that its vapor phase could consist of neutral ion pair "molecules" held together by a strong hydrogen bond, which is in contrast with very recent findings that in an FT-ICR MS experiment, the vapor consists solely of neutral molecules of tmg and HCl. This highlights the significant differences in the conditions of the experimental techniques, which can induce different speciation. In the FT-ICR MS measurements,[9] the species in the gas phase are recorded instantaneously under ultrahigh vacuum, in conditions not dissimilar to a reduced pressure distillation. The situation is different in the Raman technique,[10] where the spectra are collected over a period of several hours at a much higher pressure, the equilibrium vapor pressure of the liquid, revealing a time-averaged composition of the species present in the gas phase. It was clearly important to investigate if the species recorded in the gas phase depend on the experimental conditions used in each method. Therefore, in this study, we tested by Raman spectroscopy which species would be found to be present in the vapor phase over liquid [Hmim][O$_2$CCH$_3$]. The main advantage of Raman spectroscopy over other analytical tech-

* To whom correspondence should be addressed. E-mail: rwb@kemi.dtu.dk.
† Technical University of Denmark; www.kemi.dtu.dk.
‡ Universidade Nova de Lisboa; www.itqb.unl.pt.
§ The Queen's University of Belfast; quill.qub.ac.uk.
⊥ Massachusetts Institute of Technology; web.mit.edu.

niques is that it can identify discrete species in situ. The measurements can be performed on samples in any phase, directly in sealed ampules (or other kinds of closed vials) due to the transparency of most glasses and window materials.

In this work, we present the results of the first spectroscopic study on the composition of the vapor of [Hmim][O$_2$CCH$_3$] as a representative example of a protic ionic liquid in equilibrium with its vapor. Although Raman spectra of samples in the gas phase are often very difficult to record as the Raman effect is weak (probably only 10^{-8} of the photons hitting the sample are scattered), we successfully recorded the spectrum of the gas phase over [Hmim][O$_2$CCH$_3$]. The species in the gas phase were identified, and the bands were assigned. It was found that the gas phase of [Hmim][O$_2$CCH$_3$] predominantly consists of neutral molecules, 1-methylimidazole and ethanoic acid, with the acid being mainly in its monomeric form. The spectra were compared to the theoretical spectra predicted by ab initio DFT/B3LYP calculations with a Gaussian 6-311G+(d,p) basis set. These results add detailed confidence to our present knowledge of the composition of the gas phase over ionic liquids.

Experimental Section

Materials. [Hmim][O$_2$CCH$_3$] was prepared by mixing equimolar amounts of ethanoic acid (acetic acid >99.8%, Sigma-Aldrich) with 1-methylimidazole (99%, Aldrich) and stirring at room temperature for 2 h. The ionic liquid was then purified by drying in vacuo; the stoicheiometry was verified by ^{1}H NMR spectroscopy and elemental analysis (see Supporting Information).

Samples for the measurements were prepared in an inert atmosphere drybox by placing the compound (~500 mg) in a small Pyrex glass vial with a cap (for FT Raman measurements) or a small cylindrical glass vial of 10 mm internal diameter (for dispersive Raman measurements), flame-sealed under vacuum (<1 Pa) or under a N$_2$ atmosphere (1 bar).

Ab Initio Calculations. The ab initio quantum chemical molecular orbital calculations were performed by use of a GAUSSIAN 03W program package[11] on a 3 GHz personal computer (Pentium R4 processor) operated under Windows XP. Estimated geometries of the molecular ions, assumed to be in hypothetical gaseous free states with minimal symmetry, were used as input. The total geometric/conformational energies were minimized by use of Hartree−Fock/Kohn−Sham density functional theory (DFT) procedures at a level of approximation limited by use of the restricted-spin Becke's three-parameter hybrid exchange functional (B3), Lee−Yang−Parr correlation and exchange functionals (LYP), and with Pople's polarization split valence Gaussian basis set functions, augmented with d- and p-type polarization functions and diffuse orbitals on non-hydrogen orbitals (B3LYP, 6-311+G(d,p)). The GAUSSIAN 03W software was used as implemented, with the modified GDIIS algorithm and tight optimization convergence criteria. Optimized results are given as sums of electronic and thermal free energies in atomic units (au or Hartree), not including the zero-point energy corrections. The vibrational frequencies and eigenvectors for each normal mode were calculated without adjusting force constants. MP2-type calculations were attempted, giving essentially similar structural results, but the time to calculate spectra was impractically long.

Raman Spectroscopy. Dispersive DILOR-XY and Fourier-Transform Bruker-IFS66 FRA-106 Fourier-Transform Raman spectrometers were used, as described elsewhere.[12−15] The FT-Raman spectra were obtained on the Bruker spectrometer using a 1064 nm NIR Nd:YAG laser (<100 mW) and a liquid-
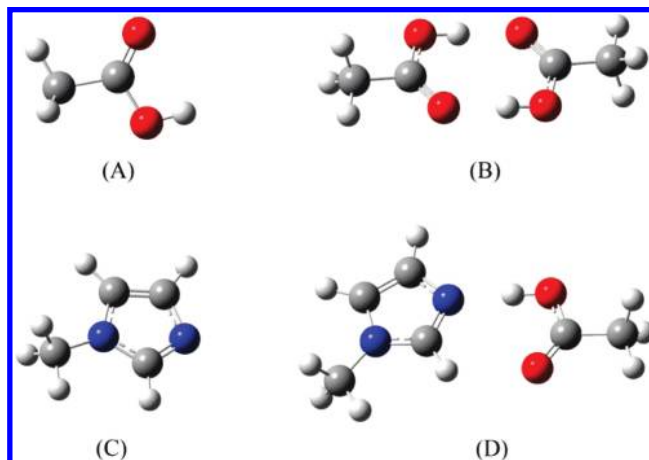

Figure 1. Optimized geometries of (A) ethanoic acid, (B) its dimer, (C) 1-methylimidazole, and (D) a {(mim)(HO$_2$CCH$_3$)} complex (starting from [Hmim]$^+$ and [O$_2$CCH$_3$]$^-$ ions) obtained by DFT/B3LYP calculations with Gaussian 6-311G+(d,p) basis sets.
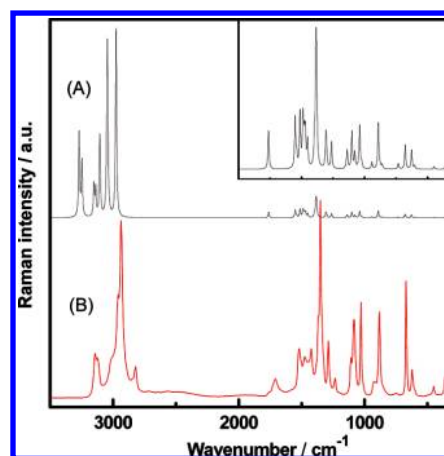

Figure 2. Calculated Raman spectrum of (A) the {(mim)(HO$_2$CCH$_3$)} complex, compared to the (B) experimental FT-Raman scattering of the ionic liquid, measured at 23 °C with a 1064 nm excitation wavelength. In the inset, the magnified (intensity) lower frequency region of the calculated spectrum is shown. The spectrum was calculated by the DFT/6-311G+(d,p)/B3LYP Gaussian modeling. Curves have been arbitrarily scaled and shifted.

nitrogen-cooled Ge diode detector, directly on small sealed glass tubes. More than 400 scans were collected in a 100−3500 cm^{-1} (Stokes) range, at approximately 23 °C. The resulting data were averaged, followed by apodization and fast-Fourier-transformation to obtain a resolution of ~2 cm^{-1} and a precision better than 1 cm^{-1}. The spectra were not corrected for (small) intensity changes in detector response versus wavelength.

The dispersive Raman spectra of the gas phase were collected separately in sealed glass vials using a DILOR-XY 800 mm focal length spectrometer with a macro entrance. Spectra were excited horizontally with a doubled Nd:YVO$_4$ laser (~2 W, vertically polarized). The Rayleigh scattered light was filtered by a double premonochromator, giving approximately a 100 cm^{-1} cutoff. The Raman light was dispersed by an 1800 lines mm^{-1} grating and focused on a highly sensitive CCD detector, cooled to ~140 K by liquid N$_2$. The slits were set to 600 μm, corresponding to a resolution of about 6 cm^{-1}. The precision was about 1 cm^{-1} for sharp bands, achieved by calibration of the wavenumber scale with Raman lines from liquid cyclohexane to within ±1 cm^{-1}.[16] The spectra were recorded in several

10836 *J. Phys. Chem. A, Vol. 114, No. 40, 2010*

Berg et al.

TABLE 1: Calculated Vibrational Spectra for the 1-Methylimidazole−Ethanoic Acid Complex and Corresponding Assignments

mode no.	wavenumber shifts/cm^{-1}	infrared absorption/ km mole^{-1}	Raman activity/ Å^4 AMU^{-1}	depolarization ratio	description of normal mode (assignment)[a,d]
1	36.5	6.23	0.18	0.75	inter bend oopl
2	54.3	0.71	1.21	0.75	inter bend oopl
3	63.5	0.16	0.14	0.75	CH$_3$ twist
4	66.7	7.72	0.04	0.74	inter OH str
5	69.6	0.36	0.56	0.75	CH$_3$ twist
6	108.9	0.14	1.87	0.75	inter bend oopl
7	127.5	1.82	0.31	0.69	inter bend ipl
8	167.3	23.28	0.20	0.50	inter NH str
9	215.8	1.63	1.09	0.75	N−CH$_3$ wag
10	357.7	0.03	0.89	0.75	N−CH$_3$ rock
11	449.1	18.90	0.72	0.73	C−CH$_3$ rock
12	602.6	1.20	0.92	0.75	skeleton^b def oopl
13	625.9	5.04	0.22	0.75	ring def oopl
14	627.0	11.44	4.93	0.60	CO$_2$ sci + CC str
15	669.3	10.72	0.06	0.75	ring def oopl
16	677.8	5.80	6.55	0.17	N−CH$_3$ str + NC$_2$ sci
17	732.5	41.62	1.51	0.75	CH wag
18	860.5	24.88	1.08	0.75	CH wag
19	875.6	8.49	0.68	0.75	CH wag
20	891.0	9.27	12.50	0.09	CCO sym str
21	941.7	24.41	1.81	0.73	ring def ipl
22	1023.4	24.27	1.53	0.66	CH$_3^b$ def + CO str
23	1039.2	17.48	11.61	0.19	ring def ipl
24	1052.6	71.31	0.27	0.75	OH wag + CH$_3^b$ def
25	1067.3	15.72	0.16	0.75	skeleton^b def oopl
26	1078.2	19.28	4.30	0.28	CH$_3^c$ def + NC str
27	1101.3	26.26	10.03	0.28	CH rock
28	1138.2	69.69	4.89	0.36	CH rock + NC str
29	1145.9	0.14	0.67	0.75	CH$_3^c$ def
30	1262.2	19.41	7.20	0.60	CH rock + NC str
31	1301.9	275.40	4.52	0.71	skeleton^c def ipl
32	1307.5	40.15	8.08	0.40	skeleton^b def ipl
33	1380.6	0.85	20.98	0.23	skeleton^c def ipl + CH$_3^b$ umbrella + OH rock
34	1386.1	0.82	26.37	0.09	skeleton^c def ipl + CH$_3^b$ umbrella + OH rock
35	1397.7	87.37	6.48	0.14	CH$_3^b$ umbrella + OH rock
36	1452.6	14.75	7.15	0.72	CH$_3^c$ umbrella
37	1470.3	20.95	9.15	0.52	CH$_3^b$ def + OH rock
38	1479.0	9.05	6.96	0.75	CH$_3^b$ def
39	1488.0	10.82	8.76	0.75	CH$_3^c$ def
40	1491.6	6.31	6.35	0.26	OH rock
41	1512.7	11.36	14.71	0.70	CH$_3^c$ def
42	1538.9	52.09	3.35	0.56	ring def ipl +CH$_3^c$ umbrella
43	1551.2	6.15	13.45	0.10	ring def ipl + CH$_3^c$ def + OH rock
44	1762.4	312.64	10.37	0.16	skeleton^b def ipl
45	2975.4	2493.05	334.19	0.38	OH str
46	3043.0	26.98	204.42	0.04	CH$_3^c$ sym str
47	3047.4	6.75	170.56	0.01	CH$_3^b$ sym str
48	3104.2	14.27	87.91	0.75	CH$_2^c$ asym str
49	3106.5	8.08	63.50	0.75	CH$_2^b$ asym str
50	3138.2	6.96	47.97	0.74	CH$_3^c$ asym str
51	3152.0	8.32	55.61	0.72	CH$_3^b$ asym str
52	3246.9	1.01	60.48	0.73	CH str ooph
53	3248.9	23.23	42.13	0.17	CH str ooph
54	3269.6	1.73	149.81	0.15	CH str iph

[a] Abbreviations for approximation of vibration: asym = asymmetric, bend = bending, def = deformation, inter = intermolecular, rock = rocking, sci = scissoring, str = stretching, sym = symmetric, twist = twisting, wag = wagging. [b] Ethanoic acid. [c] 1-Methylimidazole. [d] Gaussian03W DFT B3LYP 6-311+G(d,p), energy for {(mim)(HO$_2$CCH$_3$)} complex = −494.78712954 au, dipole moment = 4.4355 D, and no imaginary frequencies.

overlaid sections that were combined after removal of cosmic spikes. A broad fluorescent background was subtracted when necessary.

Results and Discussion

Ab Initio Calculations. The ab initio self-consistent quantum mechanical DFT functional methods with the B3LYP basis sets have proven to be well-suited to reasonably model the molecular structures and vibrational spectra of ionic liquids. Although these calculations usually are run on isolated ions, neglecting the presence of any cation−anion interactions, the results are obtained to a reasonable approximation. In this study, however, we performed calculations on [Hmim][O$_2$CCH$_3$] using an ion pair as a model because a strong interaction between the ions was expected. The geometries and spectra were calculated using the GAUSSIAN 03W software[11] with the B3LYP/DFT/6-

Raman Study of the Vapor Phase of [Hmim][O₂CCH₃]

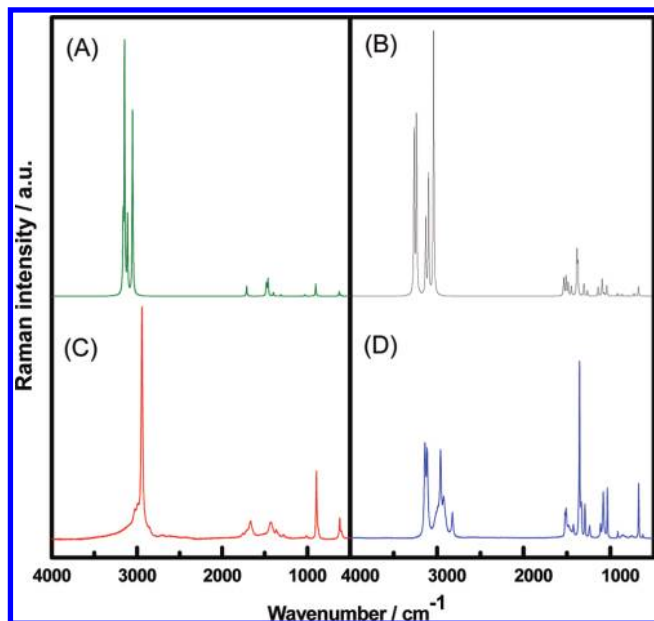*J. Phys. Chem. A, Vol. 114, No. 40, 2010* **10837**

Figure 3. Calculated Raman spectra of (A) ethanoic acid in the dimeric form and (B) 1-methylimidazole, compared to the experimental spectra for (C) liquid ethanoic acid and (D) liquid 1-methylimidazole measured at 23 °C with a 514.5 nm excitation wavelength. The spectra have been calculated by DFT/6-311G+(d,p)/B3LYP Gaussian modeling. Curves have been arbitrarily scaled and shifted.

Figure 4. Experimental Raman spectra of the vapor phase of (A) 1-methylimidazole (measured at 150 °C with a 532 nm excitation wavelength) and (B) ethanoic acid (measured at 200 °C with a 514.5 nm excitation wavelength) compared to the spectra of (C) the vapor over [Hmim][O₂CCH₃] measured at 200 °C with a 514.5 nm excitation wavelength and (D) the [Hmim][O₂CCH₃] ionic liquid measured at 23 °C with a 532 nm excitation wavelength. Curves have been arbitrarily scaled and shifted. The band at 2145 cm^{-1} is presumably due to traces of CO.

$311+G(d,p)$ basis set, and the results are shown in Figures 1 and 2. The bands were assigned to normal modes on the basis of potential energy distribution analysis, and the results are presented in Table 1. Additionally, the molecular structures and vibrational spectra of ethanoic acid and 1-methylimidazole molecules were calculated, and the results are presented in Figures 1, 3, and 5 and Tables 2−4. Previously, ethanoic acid in the gas phase was reported to exist as a mixture of monomeric and dimeric forms.[17] Thus, calculations on both forms of the acid were performed. The Gaussian minimum energies are given in the tables, and we note that a free ethanoic acid dimer was stabilized relative to two monomers by an amount of 0.02499714 au (65.63 kJ mol^{-1}). Also, it can be seen (Figure 5) that the most noticeable difference in the Raman spectra of the two forms is the presence of a band, calculated at ~3760 cm^{-1}, which appears only in the spectrum of the monomeric form and was assigned to the stretching vibration of the OH group of the isolated acid. Other characteristics of the monomer appeared at 859 and 1818 cm^{-1}, assignable to CC and CO stretching vibrations, respectively. These bands are shifted in the spectrum of the dimer to 902 and 1713 cm^{-1}, respectively.

Experimental Vibrational Spectra. In Figure 2, a comparison between the experimental and the calculated Raman spectra of liquid [Hmim][O₂CCH₃] is presented. The measurement was carried out using the FT-Raman instrument due to the strong fluorescence of the ionic liquid. The experimental spectrum is not in perfect agreement with the calculated one, and a major difference in the intensities of the bands can be observed. However, when scaling up the lower-frequency region of the calculated spectrum (Figure 2), one can notice that the position and relative intensities of the bands are, in principle, in good agreement with the experiments. To check the accuracy of the prediction model, calculations were performed also on the starting materials, ethanoic acid and 1-methylimidazole. Experimental spectra of both liquids were collected using the dispersive Raman setup. The obtained results (Figure 3) show a similar trend to that for the ionic liquid. In both cases, the
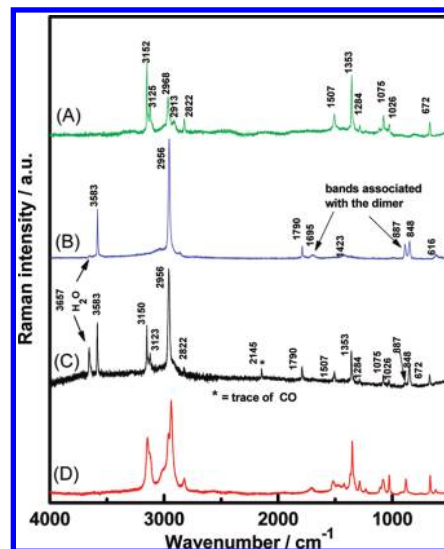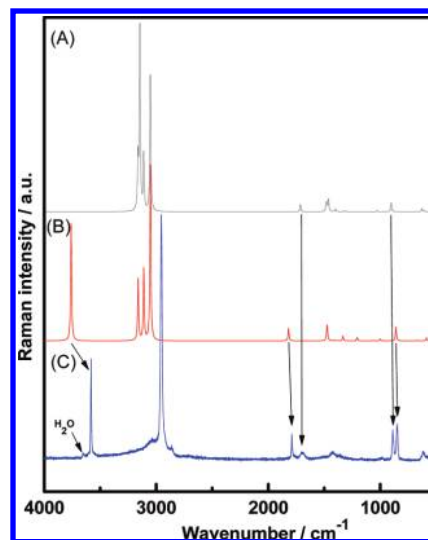

Figure 5. Calculated Raman spectra of ethanoic acid in (A) a dimeric and (B) a monomeric form, compared to (C) the experimental spectrum of the vapor over pure ethanoic acid at 200 °C measured with a 514.5 nm excitation wavelength. The spectra have been calculated by DFT/6-311G+(d,p)/B3LYP Gaussian modeling. Curves have been arbitrarily scaled and shifted.

relative intensities of the bands in the lower- and higher-frequency regions of the calculated spectra are somewhat perturbed. Nevertheless, the shape and position of the bands are in good agreement with the experimental spectra. This situation is not unusual; very often in DFT studies, when comparing calculated and experimental bands, one often gets nonperfect fits that however resemble each other. It is mainly caused by the lack of good modeling of the orbitals and model limitations in describing the internal and external interactions between the ions and the surroundings. Scaling factors can be used to get better agreement, but such a procedure was not used in this work; Tables 1−4 thus show unscaled results. The assignments given in these tables have been read off from the

TABLE 2: Calculated Vibrational Spectra for Monomeric Ethanoic Acid, Assignments, and Experimental Raman Bands for the Gas Phase at 200 °C

mode no.	wavenumber shifts/cm^{-1}	infrared absorption/ km mole^{-1}	Raman activity/ Å^4 AMU^{-1}	depolarization ratio	description of normal mode (assignment)^{a,b}	Raman bands observed for gas at 200 °C/cm$^{-1\,c}$
1	53.4	0.28	0.18	0.75	CH$_3$ twist	
2	424.8	4.80	0.32	0.75	CCO sci	
3	542.6	33.56	1.98	0.75	skeleton def oopl	
4	585.9	38.19	2.47	0.75	CO$_2$ sci	
5	661.2	98.55	0.35	0.75	skeleton def oopl	616 w
6	859.2	4.61	11.29	0.08	CC sym str	
7	999.1	77.76	1.56	0.61	skeleton def ipl	848 m
8	1067.0	8.14	0.34	0.75	CH$_3$ def + CC wag	
9	1204.8	227.67	2.65	0.75	skeleton def ipl	
10	1332.1	38.25	3.97	0.65	HOC sci + CH$_3$ umbrella	
11	1407.7	50.96	0.61	0.30	CH$_3$ umbrella	
12	1472.2	16.69	8.59	0.67	CH$_3$ def	
13	1476.5	10.58	6.59	0.75	CH$_3$ def	1423 w br
14	1818.4	367.04	10.16	0.29	CO str + HOC sci + CH$_3$ def	1423 w br
15	3051.6	1.64	142.44	0.01	CH$_3$ sym str	1790 m
16	3111.0	4.13	57.88	0.75	CH$_2$ asym str	2956 vs
17	3161.1	5.02	50.20	0.70	CH$_3$ asym str	3036 vw
18	3759.5	63.00	95.60	0.24	OH str	3583 s

^{a} Abbreviations for approximation of vibration: asym = asymmetric, def = deformation, sci = scissoring, str = stretching, sym = symmetric, twist = twisting, wag = wagging. ^{b} Gaussian03W DFT B3LYP 6-311+G(d,p), energy for monomeric ethanoic acid = −229.16476129 au, dipole moment = 1.7443 D, and no imaginary frequencies. ^{c} Codes for experimental band intensity: m = medium, s = strong, sh = shoulder, sp = sharp, v = very, w = weak, br = broad.

eigenvectors for the normal modes displayed on a computer screen to identify visually the dominating motions.

In the next step, the vapor over the [Hmim][O$_2$CCH$_3$] liquid was studied. Some of the obtained results are shown in Figure 4. It can be clearly observed that the spectrum of the liquid [Hmim][O$_2$CCH$_3$] (D) varies considerably from that of its gas phase (C), suggesting a difference in the speciation within the two phases.

According to Earle et al.,[4] in the case of liquid [Hmim]-[O$_2$CCH$_3$], the vaporization involves a proton-transfer mechanism with formation of two volatile, neutral molecules. To check if this really is the case, the Raman spectra of the different vapor phases, the starting materials 1-methylimidazole and ethanoic acid and the 1:1 mixture, were recorded (Figure 4). As expected, the gas-phase spectrum of the ionic liquid (C) matches quite convincingly to the sum of those obtained for the reagents, that is, 1-methylimidazole (B) and ethanoic acid (A), confirming unambiguously that the vaporization process for [Hmim]-[O$_2$CCH$_3$] occurs via formation of neutral molecules, according to eq 2.

$$[Hmim][O_2CCH_3](l) \rightleftharpoons mim(l) + HO_2CCH_3(l) \rightleftharpoons$$
$$mim(g) + HO_2CCH_3(g) \quad (2)$$
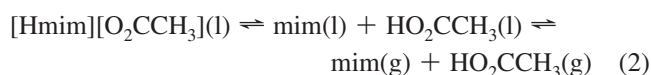
These findings are in perfect agreement with the results reported by Leal et al.,[9] where the gas phase of [Hmim]-[O$_2$CCH$_3$] was studied by means of FT-ICR MS. It should be stressed, though, that the experimental conditions differ considerably from those in the Raman experiment, which mimic the vapor−liquid equilibrium conditions of a protic ionic liquid in a more realistic manner (higher concentrations, no ionization, and measurements over a prolonged time scale).

As previously mentioned, pure ethanoic acid exists in the gas phase as a mixture of monomeric and dimeric forms in equilibrium (eq 3)

2CH$_3$COOH $\rightleftharpoons$ CH$_3$—⟨O-----H—O / O—H-----O⟩—CH$_3$ (3)
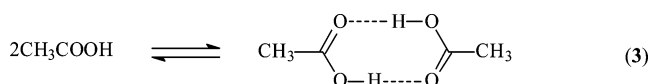
This equilibrium is temperature-dependent; dissociation constants of the reverse reaction range from a value of 10^{-3} bar at 298 K, to about 2 bar at 393 K, and to above 30 bar at 473 K.[17-19] This means that under the vapor−liquid working conditions of the Raman experiments performed for the protic ionic liquid (473 K; a moderately high temperature) and the dilution effect on the ethanoic acid by virtue of the presence of the base (mim), the predominant species of ethanoic acid in the vapor phase should be the monomer (assuming negligible interactions between mim and HO$_2$CCH$_3$ and mim and (HO$_2$CCH$_3$)$_2$ in the gas phase).

In order to check this prediction, first, the calculated spectra (both the monomer and dimer) were compared to the experimental Raman spectra of the vapor phase of pure ethanoic acid, and the results are shown in Figure 5. These results show that both forms are present in the gaseous phase of pure ethanoic acid. Bands characteristic of the monomer appear at 848, 1790, and 3583 cm^{-1} (calculated: 859, 1818, and 3760 cm^{-1}), and those for the dimer are at 887 and 1695 cm^{-1} (calculated: 902 and 1713 cm^{-1}). The main difference between the spectra of these forms is the band at 3583 cm^{-1} (calculated: 3760 cm^{-1}), assigned to the stretching vibration of the OH group in the monomeric molecule. Therefore, the spectra also show that the predominant species are the monomers, despite the dimeric molecule being more stable than two isolated monomeric molecules by 0.02499714 au (65.63 kJ mol^{-1}) (see Tables 2 and 3), and this does compensate for the entropic penalty necessary to unite two molecules in the gas phase and shift the equilibrium in eq 3 to the right-hand-side.

The temperature behavior of the gaseous phase of pure ethanoic acid is shown in Figure 6. The relative change in the two bands at 800−900 cm^{-1} reflects the shift in the equilibrium in eq 3, with the monomeric form becoming even more predominant at higher temperatures (see next paragraph).

Now, refocusing on the experimental spectrum of the vapor over the [Hmim][O$_2$CCH$_3$] liquid, its temperature dependence is shown in Figure 7. We see a considerable increase in the signals of the components with temperature. The band at 3583 cm^{-1} is easily identified in the gas over [Hmim][O$_2$CCH$_3$], indicating the presence of ethanoic acid in its monomeric form. Weak bands characteristic of the dimeric form are also present

TABLE 3: Calculated Vibrational Spectra for the Dimeric Ethanoic Acid Complex and Assignments

mode no.	wavenumber shifts/cm^{-1}	infrared absorption/ km mole^{-1}	Raman activity/ Å^4 AMU^{-1}	depolarization ratio	description of normal mode (assignment)[a,b]
1	39.4	4.27	0.00	0.74	CH$_3$ twist
2	45.9	0.00	0.77	0.75	CH$_3$ twist
3	65.8	1.36	0.00	0.72	CH$_3$ twist
4	76.7	0.04	0.00	0.73	inter twist oopl
5	120.0	0.00	0.55	0.75	inter bend oopl
6	159.3	0.00	0.38	0.65	inter bend ipl
7	172.7	31.25	0.00	0.75	inter OH str ooph
8	174.7	0.00	0.16	0.07	inter OH str iph
9	442.5	0.00	1.70	0.53	skeleton def iph ipl
10	479.6	49.70	0.00	0.75	skeleton def ooph ipl
11	599.4	0.44	0.00	0.53	skeleton def ooph oopl
12	602.7	0.00	1.29	0.53	skeleton def iph oopl
13	625.5	0.00	7.56	0.75	CO$_2$ sci iph
14	633.2	42.27	0.00	0.63	CO$_2$ sci ooph
15[c]	901.5	0.00	20.17	0.75	CC str iph + CO$_2$ sci iph
16	904.5	6.04	0.00	0.73	CO$_2$ sci ooph + CH$_3$ str ooph
17	957.7	0.00	0.32	0.75	OH wag iph
18	995.2	219.89	0.00	0.32	OH wag ooph
19	1028.6	0.00	2.09	0.73	CH$_3$ def
20	1031.9	37.68	0.00	0.75	CH$_3$ def
21	1069.4	0.00	0.29	0.75	CH$_3$ def
22	1071.6	15.87	0.00	0.48	CH$_3$ def
23	1312.3	0.00	2.50	0.67	skeleton def iph
24	1326.9	417.71	0.00	0.75	skeleton def ooph
25	1393.6	49.57	0.00	0.75	CH$_3$ umbrella ooph + OH rock ooph
26	1399.0	0.00	5.98	0.61	CH$_3$ umbrella iph + OH rock iph
27	1454.2	145.01	0.00	0.75	skeleton def ooph
28	1461.9	0.00	27.90	0.41	skeleton def iph
29	1470.9	68.10	0.00	0.75	CH$_3$ def ooph + OH rock ooph
30	1477.3	0.00	13.74	0.75	CH$_3$ def
31	1477.4	21.22	0.00	0.75	CH$_3$ def
32	1482.6	0.00	13.50	0.48	skeleton def inph
33[d]	1712.7	0.00	16.36	0.11	CO str iph + HOC sci ihp + CH$_3$ def
34	1762.2	867.22	0.00	0.75	CO str ooph + HOC sci ooph + CH$_3$ def
35	3052.1	0.00	307.05	0.01	CH$_3$ sym str iph
36	3052.2	2.49	0.00	0.05	CH$_3$ sym str ooph
37	3111.5	0.00	126.76	0.75	CH$_2$ asym str iph
38	3111.6	7.20	0.00	0.71	CH$_2$ asym str ooph
39	3146.3	0.00	412.57	0.28	OH str iph + CH str iph
40	3161.3	18.58	0.00	0.75	CH asym str ooph
41	3162.7	0.00	110.35	0.68	CH$_3$ asym str iph + OH str iph
42	3242.1	3028.58	0.00	0.75	OH str ooph

[a] Abbreviations for approximation of vibration: asym = asymmetric, bend = bending, def = deformation, inter = intermolecular, rock = rocking, sci = scissoring, str = stretching, sym = symmetric, twist = twisting, wag = wagging. [b] Gaussian03W DFT B3LYP 6-311+G(d,p), energy for dimeric ethanoic acid complex = −458.35451972 au, dipole moment = 0.2235 D, and no imaginary frequencies. [c] Observed as a medium-intensity Raman band at 887 cm^{-1} in the gas phase at 200 °C. [d] Observed as a weak broad Raman band at 1695 cm^{-1} in the gas phase at 200 °C.
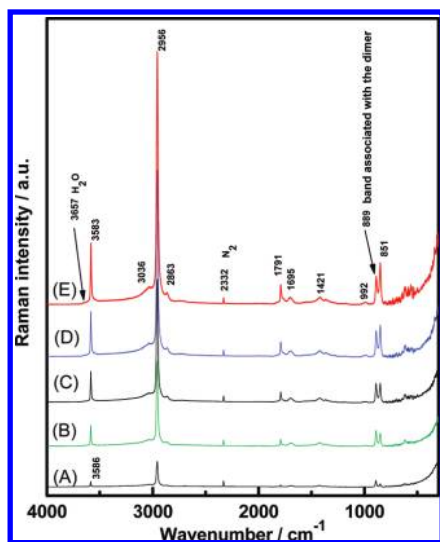

Figure 6. Raman spectra of the gas phase over ethanoic acid versus temperature, measured with a 532 nm excitation wavelength. From the bottom, traces are shown for temperatures of (A) 130, (B) 180, (C) 200, (D) 220, and (E) 240 °C. The ampules contained about 1 bar of dinitrogen, giving rise to the bands at 2332 cm^{-1} that were used to scale (normalize) the spectra mutually. The spectra have been arbitrarily shifted. The boiling point of ethanoic acid is ∼118 °C; therefore, all ampules had considerable overpressures.
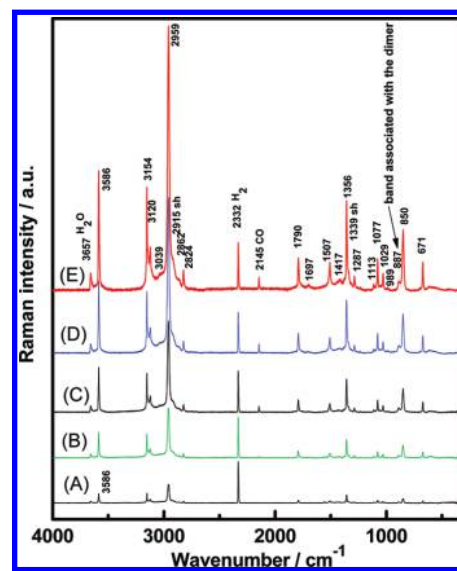

Figure 7. Raman spectra of the gas phase over [Hmim][O₂CCH₃], measured with a 532 nm excitation wavelength. Temperatures from the bottom were (A) 150, (B) 180, (C) 200, (D) 220, and (E) 240 °C. The ampules contained about 1 bar of dinitrogen, giving rise to the bands at 2332 cm^{-1} that were used to scale (normalize) the spectra. The spectra have been arbitrarily shifted. The band at 2145 cm^{-1} is presumably due to adventitious CO.

TABLE 4: Calculated Vibrational Spectra for 1-Methylimidazole, Assignments, and Experimental Raman Bands for the Gas Phase at 150 °C

mode no.	wavenumber shifts/cm^{-1}	infrared absorption/ km mole^{-1}	Raman activity/ Å^4 AMU^{-1}	depolarisation ratio	description of normal mode (assignment)^{a,b}	Raman bands observed for gas at 150 °C/cm$^{-1\,c}$
1	76.5	0.09	0.28	0.75	CH$_3$ twist	
2	207.1	1.06	1.43	0.75	N−CH$_3$ wag	
3	348.0	0.60	0.65	0.74	N−CH$_3$ rock	
4	620.6	6.65	0.22	0.75	ring def oopl	
5	671.6	14.76	0.05	0.75	ring def oopl	
6	675.2	3.78	6.86	0.21	N−CH$_3$ str + CNC sci	672 m
7	727.0	36.82	1.92	0.75	CH wag oopl	803 w br
8	810.9	33.58	0.33	0.75	CH wag oopl	
9	867.1	2.33	1.39	0.75	CH wag oopl	
10	917.1	7.41	2.03	0.75	skeleton def ipl	
11	1041.5	9.73	7.39	0.13	skeleton def ipl	1026 w
12	1072.0	11.76	1.82	0.20	CH$_3$ def + CN str	
13	1094.9	12.90	12.45	0.26	CH rock	1075 m
14	1140.6	20.91	5.71	0.48	CH rock + CN str	1112 vw
15	1142.9	0.14	0.74	0.75	CH$_3$ def	1234 vw
16	1264.1	20.77	3.69	0.74	CH rock + CN str	1284 w
17	1304.7	24.54	8.51	0.41	CH rock + CN str	1335 vw sh
18	1375.2	3.02	20.33	0.06	CNC asym str + CH$_3$ def	1353 s
19	1386.1	0.87	30.72	0.18	CNC asym str + CH rock	1375 vw
20	1450.7	17.02	6.82	0.73	CH$_3$ umbrella	
21	1487.0	9.85	9.40	0.75	CH$_3$ def	1431 vw br
22	1511.3	6.93	14.04	0.59	CH$_3$ def + CC str	
23	1534.1	65.89	3.21	0.29	ring def ipl + CH$_3$ umbrella	
24	1538.3	4.11	10.82	0.10	CH$_3$ def + CC str + CH rock	1507 m
25	3037.7	47.71	187.96	0.03	CH$_3$ sym str	2822 m
26	3096.6	17.54	85.22	0.75	CH$_2$ asym str	2913 w
27	3129.3	9.36	54.22	0.73	CH$_3$ asym str	2968 s
28	3233.6	3.51	49.59	0.35	CH str	3105 w sh
29	3237.3	3.05	91.37	0.47	CH str	3125 m
30	3263.7	1.93	115.54	0.15	CH str	3152 vs

^{a} Abbreviations for approximate vibrations: asym = asymmetric, def = deformation, rock = rocking, sci = scissoring, str = stretching, sym = symmetric, twist = twisting, wag = wagging. ^{b} Gaussian03W DFT B3LYP 6-311+G(d,p), energy for 1-methylimidazole = −265.60200413 au, dipole moment = 4.2740 D, and no imaginary frequencies. ^{c} Codes for experimental band intensity: m = medium, s = strong, sh = shoulder, sp = sharp, v = very, w = weak, br = broad.

in the spectra, for example, the bands at 1695 and 887 cm^{-1} (also clearly distinguishable) in Figure 4B, but the ethanoic acid dimer density decreases when the temperature is increased or when 1-methylimidazole is present. From that, it can be concluded that the equilibrium between the forms of ethanoic acid in the vapor of [Hmim][O$_2$CCH$_3$] is significantly shifted toward the left-hand-side in eq 3, the monomer (under given experimental conditions). It is overwhelmingly convincing to see that this expected behavior is borne out also by the Raman study.

In addition, the bands from the 1-methylimidazole molecule in the vapor (Figure 4A) can be seen clearly in the spectra from the gas phase over [Hmim][O$_2$CCH$_3$] (Figures 4C and 7).

The stabilization of the associated {(mim)(HO$_2$CCH$_3$)} complex (shown in Figure 1D) was calculated by the ab initio methods to amount to 0.02036312 au (53.46 kJ mol^{-1}) relative to a monomer ethanoic acid molecule and the 1-methylimidazole molecule (see Tables 1, 2, and 4). As this value is even smaller for that of the dimerization of ethanoic acid, it is unsurprisingly insufficient to stabilize the addition complex in the gas phase at 200 °C. Thus, the stability of {(mim)(HO$_2$CCH$_3$)} is determined by entropic considerations as the −TΔS term dominates, and essentially, a complete dissociation into neutral molecules occurs. This contrasts with the case of aprotic (totally ionized) ionic liquids, in which this last option (the dissociation into neutral molecules in the gas phase) is not possible, which means that the gas phase is essentially composed of neutral ion pairs, and the corresponding liquid phase exhibits an extremely

low vapor pressure. In the liquid phase of [Hmim][O$_2$CCH$_3$], its predominant form is as a protic ionic liquid (see eq 1) with significant association between the dissolved species. This is also reflected in our observed spectra, as shown in Figure 8. Here, we have reproduced Raman spectra of the gas phase over [Hmim][O$_2$CCH$_3$] (lower trace (B)) and the sum of mim and HO$_2$CCH$_3$, measured at 220 °C (upper trace (A)). All ampules contained dinitrogen (at about 1 bar), giving rise to the N$_2$ Q branch band at ∼2332 cm^{-1}. That band was used to scale (normalize) the spectra. The reason for the intensity sum of mim and HO$_2$CCH$_3$ (upper trace (A)) being larger than that of the gas over [Hmim][O$_2$CCH$_3$] must be explained as due to the affinity between the components forming the ionic liquid.

Summary

The Raman spectra of the vapor phase over [Hmim][O$_2$CCH$_3$] and its components were recorded and proved to be consistent with its essentially complete dissociation into neutral component molecules, ethanoic acid, and 1-methylimidazole, with the ethanoic acid being mainly in its monomeric form. The obtained spectra were compared to the ab initio calculated models with satisfactory agreement, and detailed and reliable band assignments were possible. The ab initio self-consistent quantum mechanical DFT functional methods with the chosen B3LYP/ 6-311+G(d,p) basis sets were well-suited to reasonably model the molecular ion structures and calculate vibrational spectra of these ions. The results are giving convincing support to the predictions made by Earle et al.[4] and later observations by Leal
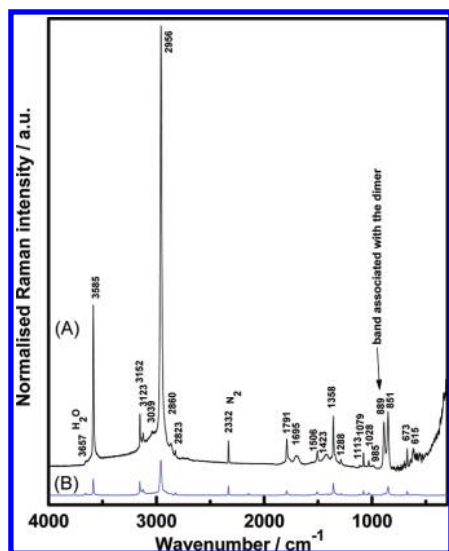
Figure 8. Comparison between (A) the sum of the Raman spectra of the gas phase over mim and HO_2CCH_3 and (B) the spectrum of the gas phase over [Hmim][O_2CCH_3], measured with a 532 nm excitation wavelength at 220 °C. The ampules also contained about 1 bar of dinitrogen, giving rise to the Q branch band at ~ 2332 cm^{-1} that was used to scale (normalize) the spectra. The spectra have been arbitrarily shifted. The band at 2145 cm^{-1} is presumably due to adventitious CO. The reason for the (A) curve (sum of scaled neat components) being more intense than the (B) curve (the gas phase over [Hmim][O_2CCH_3]) is thought to be due to the affinity between the components forming the ionic liquid.

et al.,[9] where the gas phase of [Hmim][O_2CCH_3] was studied by means of the FT-ICR MS. It is important to remember, though, that this conclusion cannot be generalized for all of the protic ionic liquids, and further studies are needed, particularly on systems derived from stronger bases.

Supporting Information Available: A supplementary table lists calculated normal coordinates and vibrational data of (a) the ethanoic acid, (b) its dimer, (c) 1-methylimidazole, and (d) the (mim)(HO_2CCH_3) complex (starting from [Hmim]$^+$ and [O_2CCH_3]$^-$ ions) obtained by DFT/B3LYP calculations with Gaussian 6-311G+(d,p) basis sets. This material is available free of charge via the Internet at http://pubs.acs.org.

References and Notes

(1) MacFarlane, D. R.; Seddon, K. R. *Aust. J. Chem.* **2007**, *60*, 3–5.
(2) Johansson, K. M.; Izgorodina, E. I.; Forsyth, M.; MacFarlane, D. R.; Seddon, K. R. *Phys. Chem. Chem. Phys.* **2008**, *10*, 2972–2978.
(3) Greaves, T. L.; Drummond, C. J. *Chem. Rev.* **2008**, *108*, 206–237.
(4) Earle, M. J.; Esperança, J. M. S. S.; Gilea, M. A.; Canongia Lopes, J. N.; Rebelo, L. P. N.; Magee, J. W.; Seddon, K. R.; Widegren, J. A. *Nature* **2006**, *439*, 831–834.
(5) Esperança, J. M. S. S.; Canongia Lopes, J. N.; Tariq, M.; Santos, L. M. N. B. F.; Magee, J. W.; Rebelo, L. P. N. *J. Chem. Eng. Data* **2010**, *55*, 3–12.
(6) Yoshizawa, M.; Xu, W.; Angell, C. A. *J. Am. Chem. Soc.* **2003**, *125*, 15411–15419.
(7) Canongia Lopes, J. N.; Rebelo, L. P. N. *Phys. Chem. Chem. Phys.* **2010**, *12*, 1948–1952.
(8) Plechkova, N. V.; Seddon, K. R. *Chem. Soc. Rev.* **2008**, *37*, 123–150.
(9) Leal, J. P.; Esperança, J. M. S. S.; Minas da Piedade, M. E.; Canongia Lopes, J. N.; Rebelo, L. P. N.; Seddon, K. R. *J. Phys. Chem. A* **2007**, *111*, 6176–6182.
(10) Berg, R. W.; Riisager, A.; Fehrmann, R. *J. Phys. Chem. A* **2008**, *112*, 8585–8592.
(11) Frisch, M. J.; Trucks, G. W.; Schlegel, H. B.; Scuseria, G. E.; Robb, M. A.; Cheeseman, J. R.; Montgomery, J. A., Jr.; Vreven, T.; Kudin, K. N.; Burant, J. C.; Millam, J. M.; Iyengar, S. S.; Tomasi, J.; Barone, V.; Mennucci, B.; Cossi, M.; Scalmani, G.; Rega, N.; Petersson, G. A.; Nakatsuji, H.; Hada, M.; Ehara, M.; Toyota, K.; Fukuda, R.; Hasegawa, J.; Ishida, M.; Nakajima, T.; Honda, Y.; Kitao, O.; Nakai, H.; Klene, M.; Li, X.; Knox, J. E.; Hratchian, H. P.; Cross, J. B.; Bakken, V.; Adamo, C.; Jaramillo, J.; Gomperts, R.; Stratmann, R. E.; Yazyev, O.; Austin, A. J.; Cammi, R.; Pomelli, C.; Ochterski, J. W.; Ayala, P. Y.; Morokuma, K.; Voth, G. A.; Salvador, P.; Dannenberg, J. J.; Zakrzewski, V. G.; Dapprich, S.; Daniels, A. D.; Strain, M. C.; Farkas, O.; Malick, D. K.; Rabuck, A. D.; Raghavachari, K.; Foresman, J. B.; Ortiz, J. V.; Cui, Q.; Baboul, A. G.; Clifford, S.; Cioslowski, J.; Stefanov, B. B.; Liu, G.; Liashenko, A.; Piskorz, P.; Komaromi, I.; Martin, R. L.; Fox, D. J.; Keith, T.; Al-Laham, M. A.; Peng, C. Y.; Nanayakkara, A.; Challacombe, M.; Gill, P. M. W.; Johnson, B.; Chen, W.; Wong, M. W.; Gonzalez, C.; Pople, J. A. *Gaussian 03*, revision B.04; Gaussian, Inc.: Pittsburgh, PA, 2003.
(12) Berg, R. W. *Ionic Liq. Chem. Anal.* **2009**, 307–354.
(13) Berg, R. W.; Deetlefs, M.; Seddon, K. R.; Shim, I.; Thompson, J. M. *J. Phys. Chem. B* **2005**, *109*, 19018–19025.
(14) Berg, R. W.; Ferre, I. M.; Schaeffer, S. J. C. *Vib. Spectrosc.* **2006**, *42*, 346–352.
(15) Brooker, M. H.; Berg, R. W.; von Barner, J. H.; Bjerrum, N. J. *Inorg. Chem.* **2000**, *39*, 4725–4730.
(16) Berg, R.; Norbygaard, T. *Appl. Spectrosc. Rev.* **2006**, *41*, 165–183.
(17) Gaufres, R.; Maillols, J.; Tabacik, V. *J. Raman Spectrosc.* **1981**, *11*, 442–448.
(18) Maier, R. W.; Brennecke, J. F.; Stadtherr, M. A. *Comput. Chem. Eng.* **2000**, *24*, 1851–1858.
(19) Taylor, M. D. *J. Am. Chem. Soc.* **1951**, *73*, 315–317.

JP1050639